Frequency dependent dielectric and mechanical behavior of elastomers for actuator applications

Martin Molberg,[1,2,a] Yves Leterrier,[2] Christopher J. G. Plummer,[2] Christian Walder,[1] Christiane Löwe,[1] Dorina M. Opris,[1] Frank A. Nüesch,[1] Siegfried Bauer,[3] and Jan-Anders E. Månson[2]

[1]*Laboratory for Functional Polymers, Swiss Federal Laboratories for Materials Testing and Research (EMPA), Überlandstrasse 129, 8600 Dübendorf, Switzerland*

[2]*Laboratoire de Technologie des Composites et Polymères (LTC), Ecole Polytechnique Fédérale de Lausanne (EPFL), 1015 Lausanne, Switzerland*

[3]*Department of Soft Matter Physics, Johannes Kepler University, Altenberger Strasse 69, 4040 Linz, Austria*

(Received 3 June 2009; accepted 29 July 2009; published online 15 September 2009)

The low frequency mechanical and dielectric behavior of three different elastomers has been investigated by dynamic mechanical analysis and dielectric spectroscopy, with the aim of accounting for the frequency dependence of the characteristics of the corresponding dielectric elastomer actuators. Satisfactory agreement was obtained between the dynamic response of the actuators and a simple model based on the experimental data for the elastomers, assuming that the relatively large prestrains employed in the actuators to have little influence on the frequency dependence of their effective moduli. It was thus demonstrated that the frequency dependence of the actuator strain is dominated by that of the mechanical response of the elastomer, and that the frequency dependence of the dielectric properties has a relatively minor influence on the actuator performance. © *2009 American Institute of Physics*. [doi:10.1063/1.3211957]

I. INTRODUCTION

A dielectric elastomer actuator (DEA) consists of an elastomer film coated on either side with compliant electrodes. When a potential difference is applied to the electrodes, these attract each other owing to their opposite charges. Because elastomers are effectively incompressible, the resulting decrease in thickness of the DEA results in a corresponding increase in its area, as shown in Fig. 1, which provides the actuation. The very high deformability, flexibility, and energy density of DEAs, together with their low weights, are of considerable interest for a wide range of applications, including micropumps, robotics, tactile interfaces, loud speakers, medical prosthetics, sensing, and energy harvesting.[1,2] An important step in the development of DEAs was the introduction of "very high bonding" (VHB) acrylate adhesive films from 3M as the dielectric elastomer. VHB films support areal strains of over 300% and have provided the focus for much subsequent research into DEA devices.[3,4] However, there remains a huge demand for improved dielectric elastomers, particularly because of the need to reduce activation voltages (typically 4–5 kV at present) for applications such as medical implants and to avoid the costly electronics required for high voltage devices. The electrostatic pressure p that acts on the elastomer film is given by

$$p = \varepsilon\varepsilon_0 E^2 = \varepsilon\varepsilon_0\left(\frac{V}{d}\right)^2, \tag{1}$$

where ε is the dielectric constant, ε_0 is the permittivity of free space, E is the electric field, V is the applied voltage, and d is the thickness of the film.[5] The compressional strain in thickness direction is then

$$s_z = \frac{p}{Y} = \frac{\varepsilon\varepsilon_0}{Y}\left(\frac{V}{d}\right)^2, \tag{2}$$

where Y is the compression modulus in the thickness direction. Actuation is hence governed by two material parameters, ε and Y. Both are functions of the actuation frequency, the stress state and the temperature, so that a complete description of the dynamic behavior of DEAs must take these factors into account.

There have been considerable previous efforts to model the behavior of DEAs based on silicone[6,8] and VHB elastomers.[7] Kofod and Sommer-Larsen[6] carried out tensile tests directly on a simple model silicone-based actuator and were able to use an empirical description of its hyperelastic behavior to describe its response to different applied voltages and loading conditions, although no attempt was made to describe the dynamic behavior in this case. Wissler and Mazza[7] also used different empirical models for the hyper-

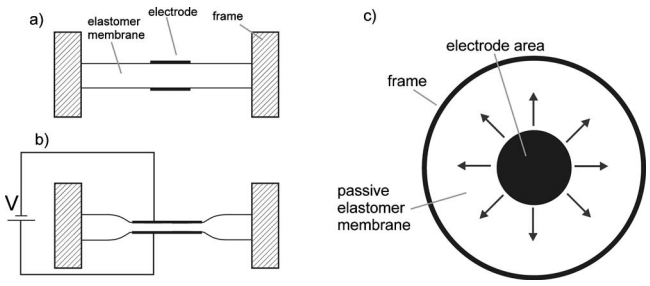

FIG. 1. Schematic cross section in (a) the nonactivated and (b) the activated states, and (c) a top view of a circular membrane actuator.

[a]Electronic mail: martin.molberg@empa.ch.

elastic response of a VHB-based actuator but were able to combine these with a strain independent relaxation function derived from tensile tests, in order to fit the time dependence of the actuator response on application of a given (constant) applied voltage and hence to successfully predict the time dependence of the response at arbitrary applied voltages.

Carpi and de Rossi[8] assumed linear elastic behavior in modeling their cylindrical silicone actuators but used independently determined values for the Young's modulus as well as for the dielectric constant (in the frequency range 10 Hz–1 GHz) rather than empirical fits to the actuator response. They subsequently argued, albeit qualitatively, that the improved performance of DEAs incorporating silicone-based composite elastomers was primarily due to an increase in dielectric constant, although their results did not imply any significant frequency dependence.[9] Finally, Palakodeti and Kessler carried out dynamic mechanical measurements on prestrained VHB films (VHB 4910 and 4905) in the frequency range 5–20 Hz and obtained a measure of the mechanical efficiency, i.e., the extent to which a DEA can convert electrical energy into mechanical energy, in terms of the loss tangent. Their results suggested an increase in efficiency at lower frequencies and higher prestrains, implying better DEA performance under these conditions, but no direct comparison was made with measurements from actual devices.[10]

The aim of the present work is to combine independently obtained data for the frequency dependence of the elastic modulus of various dielectric elastomers and the influence of relaxation after the application of a large prestrain, with data for the frequency dependence of the dielectric constant, in order to predict the low strain dynamic behavior of the corresponding actuators at frequencies below 10 Hz, the range in which actuators are required to work in most prospective applications. The results are then compared with direct observations of the actuator response in order to validate the approach, to identify the most important parameters for actuator performance, and to assess the different materials studied.

II. EXPERIMENTAL

The elastomers chosen for investigation were a 1 mm thick acrylate adhesive film (VHB 4910 from 3M), used as received, a polydimethylsiloxane (PDMS) (Neukasil RTV-23 from Swiss-Composite), and a styrene-isoprene block copolymer thermoplastic elastomer (TPE) pellets containing aliphatic oils (Betaflex from Revolflex AG). The PDMS resin was mixed with the cross-linker (A7) in the ratio 10:4. 100–200 μm thick films were prepared for dielectric spectroscopy and fabrication of the actuators by doctor blading, followed by curing for 1 day at room temperature. The TPE pellets were purified by dissolution in toluene, filtering, and drying. Films were then prepared for dielectric spectroscopy and fabrication of the actuators by first pressing a 25 mm diameter cylinder of the TPE at 160 °C and 100 kPa, and then further pressing the resulting cylinder for 15 min between two glass plates to a final thickness of 100–200 μm at 160 °C and 250 kPa. The thicknesses of the PDMS and TPE films represented a compromise between the good processability and accuracy of thickness measurements for thicker films, and the higher capacitance and lower actuation voltages for thinner films. The thicknesses were measured using a precision thickness gauge MT-30 from Heidenhain in which a caliper applies a small force to the specimen (2.2 g over a circular area with a diameter of 6 mm) and the distance between the caliper position and a reference point is detected by a displacement transducer with a resolution of 0.5 μm.

For tensile tests, the film thicknesses were increased to 1 mm for PDMS and 1.3 mm for TPE to ensure sufficient accuracy in the force measurements.

Dielectric measurements were carried out using an alpha analyzer from Novocontrol, and Novocontrol HVB 1000 or HVB 500 high voltage test interfaces at frequencies between 0.5 mHz and 1 MHz. The specimens were held between two circular 25 mm diameter copper electrodes. The dielectric constant was determined from the measured capacitance via $C=\varepsilon\varepsilon_0 A/d$, where A is the electrode area, d is the film thickness, and $\varepsilon_0=8.854\times10^{-12}$ F/m. The films were slightly compressed during the dielectric constant measurements owing to the weight of the upper electrode, but this also ensured a good contact between the films and the electrode. The thicknesses of the films were taken to equal the distance between the electrodes as determined using a micrometer gauge. The experimental error in these measurements was primarily due to errors in the film thickness determination and was estimated to be less than 10%.

The tensile tests were performed using a Zwick Z010 tensile test machine with a crosshead speed of 500 mm/min, according to ISO 37.[11] Tensile test specimens with a gauge width of 3 mm and a gauge length of 30 mm were prepared by die cutting. An optical deformation sensor (Zwick video extensometer 066975) was used to detect the tensile strain in the specimens based on measurement of the distance between two marker points placed along the axis of the tensile test bar using video cameras to 5 μm accuracy. The true stress, σ_{true}, was estimated from the axial strain, s_z, and the measured force, F_t, by assuming incompressibility, so that $\sigma_{\text{true}}=F_t/A_{\text{act}}=(s_z+1)F_t/A^0$, where A^0 is the cross-sectional area at zero strain. Three independent measurements were made for each material and the results averaged. The tangential modulus was determined from the slope of the stress-strain curves, using segmental polynomial fits to the data points, and was found to be reproducible to within ±10 kPa for a given strain.

To investigate the effect of the prestrains applied to the films used in the actuators, the test specimens were stretched to an equivalent prestrain and then left to relax for 2 h prior to resumption of the tensile test. Beyond 2 h, the relaxation modulus showed little further evolution with time and the films were therefore assumed to be in a similar state of relaxation to those in the actuators.

Oscillatory shear tests were performed on an ARES rheometer (Rheometric Scientific) in parallel plate geometry with cylindrical specimens of 25 mm diameter and 2 mm in thickness at frequencies between 0.8 mHz and 80 Hz. All the mechanical tests were carried out under controlled atmosphere at 23 °C and 50% relative humidity.

Actuator tests were performed using circular membrane actuators with prestrained films, as sketched in Fig. 1. The films were clamped to a movable square frame (original dimensions 13×13 cm^2 for TPE and PDMS, and 25×25 cm^2 for VHB), which was used to apply the chosen biaxial prestrain. VHB was prestrained to 400%, which is a standard practice and serves to reduce the film thickness and to improve electrical breakdown strength and efficiency. PDMS could not be prestrained to the same extent because the films broke at 400% strain and also showed relatively marked strain hardening, so that it was necessary to limit the prestrain to 50%. TPE was prestrained to 100%, which is well before the onset of significant strain hardening. The prestrained films were then clamped using a circular frame with an inner diameter of 30 mm. Circular electrodes (8 mm diameter) of fine carbon black powder (Ketjenblack) were applied to each side of the film. A TREK model 5/80 high voltage source, controlled by a waveform generator HP 33120A using sinusoidal signals, served as the power supply for actuator tests. The amplitude of electric field strength was chosen to give a 1% radial strain at 100 mHz, i.e., 28.07 V/μm for VHB, 22.45 V/μm for TPE, and 18 V/μm for PDMS. A video camera controlled by VIDEOEXTENSOMETER software from Messphysik GmbH, which detects the boundary between the dark electrode area and translucent surrounding area (bright-dark contrast), was used to determine the diameter of the electrode in two orthogonal directions and hence the mean radial strain in the actuators.

III. RESULTS

A. Dielectric spectroscopy

In what follows, unless mentioned otherwise, the real part (ε') of the complex dielectric constant ($\varepsilon^*=\varepsilon'-i\varepsilon''$) will be referred to simply as the dielectric constant. The dielectric constants of the different materials are shown in Fig. 2(a). In each case, the small increase at low frequencies (<100 mHz) was attributed to electrode polarization effects.[12] Over the rest of the frequency range, the dielectric constants of TPE and PDMS were nearly constant at 2 and 2.5, respectively. For VHB, on the other hand, although the dielectric constant remained close to 4.65 at intermediate frequencies, consistent with the value of 4.7 reported by Kofod *et al.*,[13] it decreased at frequencies greater than 1 kHz. These values were found to be independent of the electric field strength for electric fields of up to about 2 V/μm.

The loss factors $\tan\delta=\varepsilon''/\varepsilon'$ for the three elastomers are given in Fig. 2(b). VHB showed a considerably higher $\tan\delta$ than the other elastomers at frequencies greater than 10 Hz, for which $\tan\delta$ changed little. However, at lower frequencies, which are of interest in most actuator applications, VHB showed the lowest $\tan\delta$. The linear increases in $\tan\delta$ with decreasing frequency below 1 Hz in the shown logarithmical plot [Fig. 2(b)] reflect the limiting quasistatic conductivity value, σ_{DC}, as the conductivity depends on the imaginary part of the dielectric constant as $\sigma=2\pi f\varepsilon_0\varepsilon''$ [see Fig. 2(c)].

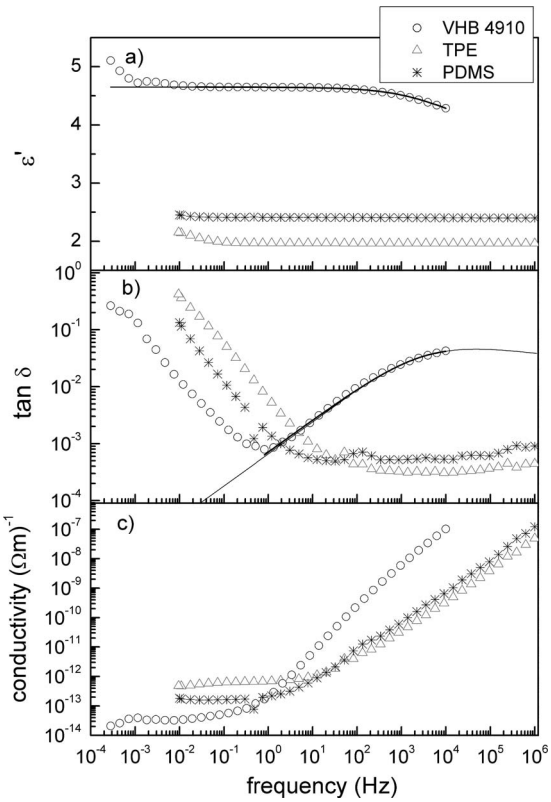

FIG. 2. (a) Dielectric constant, (b) loss factor, and (c) conductivity for the three different materials as a function of frequency.

Because an apparent maximum in $\tan\delta$ was observed for VHB in the frequency range investigated, it was possible to use the HN-equation, named after Havriliak and Negami[14]

$$\varepsilon^*(\omega)=\varepsilon_\infty+\frac{\Delta\varepsilon}{[1+(i2\pi f\tau)^\beta]^\gamma} \tag{3}$$

to fit the data at intermediate and high frequencies, as shown in Figs. 2(a) and 2(b), where ε^* is the complex dielectric constant, ε_∞ is the limiting value of the dielectric constant at high frequencies, $\Delta\varepsilon$ is the dielectric relaxation strength, τ is the relaxation time, f is the frequency of the electric field, and the exponents β and γ are the empirical parameters that define the shape of the relaxation maximum. The values of the various fitting parameters are given in Table I. Since the dielectric relaxation peak has not been fully resolved by the measurements, the fit parameters are lacking precision but are accurate enough for later discussion. The HN equation could not be applied to TPE and PDMS because of the absence of any obvious relaxation in their respective spectra.

Because conduction is a loss process for actuators, a low as possible σ is desired for dielectric elastomers. σ, derived

TABLE I. Fitting parameters for the application of the HN equation to the dielectric response of VHB.

$\Delta\varepsilon$	1.609
β	0.570
γ	0.228
ε_∞	3.04
τ	6.37×10^{-5} s

TABLE II. Quasistatic conductivity, σ_{DC}, and dielectric constant, ε'_{DC}, for the different elastomers.

	σ_{DC} ($\Omega\ m^{-1}$)	ε'_{DC}
VHB	3.5×10^{-14}	4.65
TPE	6.6×10^{-13}	2.0
PDMS	1.6×10^{-13}	2.5

from the dielectric measurements, is shown in Fig. 2(c). The power law dependence on frequency at high frequencies is consistent with the universal dielectric behavior described by Jonscher.[15] The limit of the conductivity at low frequencies, considered to represent the steady state conductivity, σ_{DC}, is given in Table II for the different materials. σ_{DC} was consistently less than $10^{-12}\ \Omega^{-1}\ m^{-1}$, but VHB showed significantly lower values than TPE and PDMS.

B. Mechanical analysis

The stress-strain curves for the elastomers determined from the standard tensile tests and the stress-strain curves obtained after straining and relaxation are shown in Fig. 3. VHB showed intermediate strain hardening and a strain at break of 680%. TPE showed the lowest strain hardening of the three materials for strains up to 700% and a strain at break of about 2500%. Finally, PDMS showed the most pronounced strain hardening at strains greater than 100% and a maximum strain of about 340%. After prestraining, a significant decrease in stress was observed during the subsequent

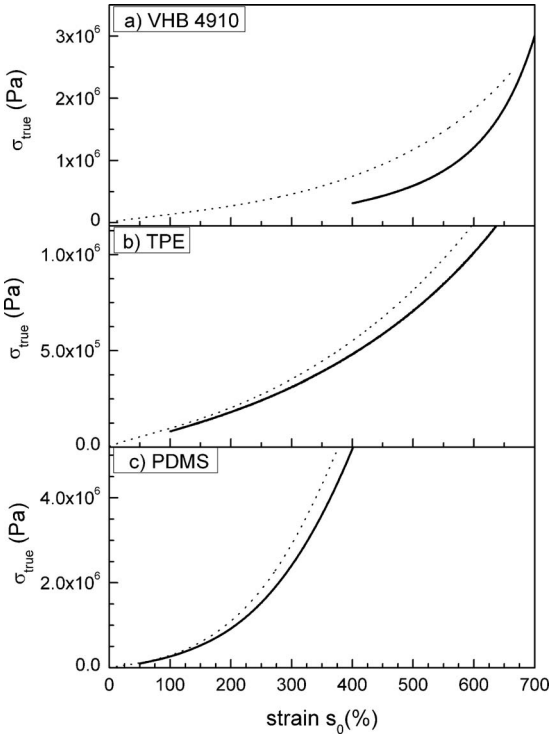

FIG. 3. Stress-strain curves for the three elastomers determined from standard tensile tests at 500 mm/min (dotted lines) and after prestraining (400% for VHB, 100% for TPE, and 50% for PDMS) and relaxation for 2 h (solid lines). The stress is corrected for areal change through straining (σ_{true}), and the strain is given relative to the original length of the sample (s_0).

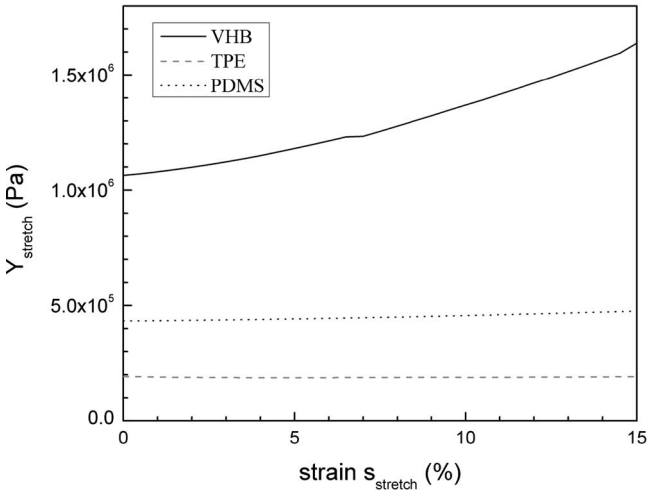

FIG. 4. Elastic modulus $Y_{stretch}$ for the three elastomers after prestraining (400% for VHB, 100% for TPE, and 50% for PDMS) and relaxation for 2 h, as a function of $s_{stretch}$.

2 h of relaxation. This decrease was more pronounced for VHB than for TPE and PDMS, although the different levels of prestrain used for each material should be borne in mind. It may also be inferred from these curves that the tangential modulus changed relatively little after relaxation compared to the initial tangential modulus in the standard tensile test.

However, the strain in an actuator is defined with respect to the dimensions of the prestrained elastomer, so that for modeling the actuator behavior it was necessary to recalculate the tangent modulus with respect to the prestrained state, i.e.,

$$Y_{stretch} = \frac{\partial \sigma_{true}}{\partial s_{stretch}}, \tag{4}$$

where $s_{stretch}=(l-l_{stretch})/l_{stretch}=(l-\lambda l_0)/(\lambda l_0)$, l is the actual length, l_0 is the gauge length in undeformed state, $l_{stretch}$ is the gauge length in the prestrained state, and λ is the deformation ratio corresponding to the prestrain (1.5, 2, and 5 for PDMS, TPE, and VHB, respectively). The evolution of $Y_{stretch}$ with $s_{stretch}$ in relaxed specimens is shown in Fig. 4. For TPE, $Y_{stretch}$ was nearly constant in the range of strains considered, while PDMS showed slight strain hardening. For VHB, on the other hand, $Y_{stretch}$ increased significantly with $s_{stretch}$, consistent with the much larger prestrains applied to this material.

The dynamic tensile behavior could not be determined directly for prestrained samples owing to their low stiffness and the limited sensitivity of the available apparatus. The frequency dependence of the tensile modulus was therefore inferred from measurements of the dynamic shear modulus, via

$$Y' = G'(2+2\upsilon), \tag{5}$$

where G' and Y' are the real parts of the dynamic shear and tensile moduli, respectively, and incompressibility (Poisson's ratio $\upsilon=0.5$) is again assumed. Results are shown in Fig. 5(a) in the frequency range 0.8 mHz–80 Hz, Y' showing an increase with increasing frequency in each case, which was particularly marked for VHB. A satisfactory analytical ex-

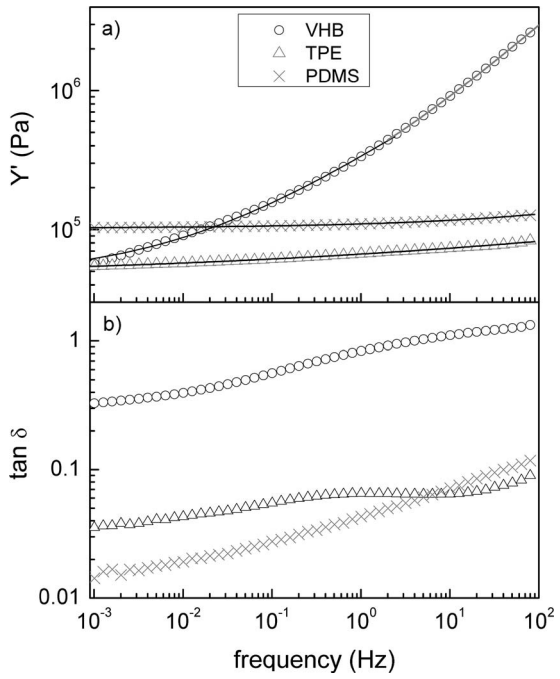

FIG. 5. Y' and tan φ of VHB, TPE, and PDMS as a function of frequency as inferred from shear modulus measurements. The curves in (a) are fits of Eq. (6) to the data.

pression for the frequency dependence of Y' could be obtained by fitting with power law of the form

$$Y' = A_0 + P \cdot f^b, \tag{6}$$

where A_0, P, and b are the empirical constants, summarized for the different materials in Table III. Use of a stretched exponential was not considered since no distinct relaxation maximum was observed in the range of frequencies investigated. To obtain a precise representation in the case of VHB, it was nevertheless necessary to use separate fits for frequencies above and below 2 Hz, as indicated in Table III.

Figure 5(b) shows the mechanical loss factor tan φ obtained from the dynamic shear modulus measurements as a function of frequency. VHB showed the highest tan φ throughout the range of frequencies investigated (0.8 mHz–80 Hz), increasing from 0.32 to 1.33. The lowest tan φ were observed for TPE, i.e., 0.015 at 0.8 mHz, but in this case tan φ increased nearly tenfold to 0.117 at 80 Hz. Thus, whereas tan φ was 0.034 for PDMS at 0.8 mHz, it showed the lowest tan φ of all the elastomers for frequencies above 5 Hz.

TABLE III. Fitting parameters for the frequency dependence of Y' inferred from dynamic shear modulus measurements for the three different elastomers.

	VHB (<2 Hz)	VHB (>2 Hz)	TPE	PDMS
A_0 (Pa)	46 282	112 814	44 674	101 947
P (Pa/Hz)^b	290 205	223 511	21 893	7 732
b	0.423	0.553	0.118	0.275

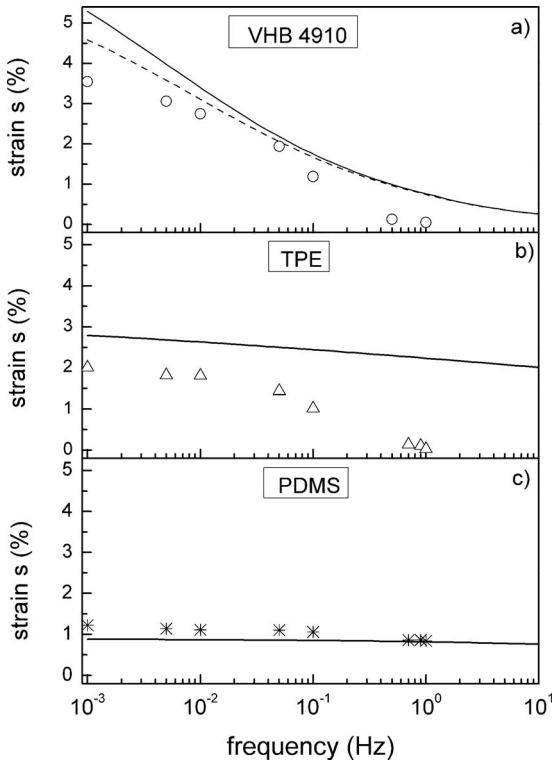

FIG. 6. Measured strain amplitude (symbols) of membrane actuators from three different elastomers as a function of the frequency of applied voltage. Note that the strain amplitude has twice the frequency of the voltage oscillation. The measured strain is compared with the strain calculated from experimentally determined material parameters (solid curves). The hatched curve in (a) was calculated taking into account the strain dependence of the modulus in VHB.

C. Actuator measurements

Circular membrane actuators were produced from all three elastomers as described in Sec. II, and tested at frequencies between 1 mHz and 1 Hz. The measured strain amplitudes for the actuators are shown as a function of frequency in Fig. 6 and compared to the amplitudes calculated as described in Sec. IV. Small strain conditions (1% at 100 mHz) were chosen to minimize thickness changes during actuation, which would lead to changes in electric field at a given voltage. In such experiments, the strain cycles at twice the frequency of the applied voltage signal because the electrostatic pressure is independent of the direction of the electric field [Eq. (1)], as pointed out by Fox and Goulbourne.[16]

The strain amplitude of actuators decreased with increasing frequency. PDMS showed the smallest decrease, the strain amplitude diminishing from 1.22% strain at 1 mHz to 0.82% at 1 Hz. TPE and VHB showed strains of 2% and 3.55%, respectively, at 1 mHz, and at 1 Hz the strains dropped to 0.05% and 0.03%, respectively. For frequencies greater than 1 Hz it was not possible to record a strain amplitude for TPE and VHB using the present setup, although the membranes continued to generate sound waves when the applied voltage oscillated in the audible frequency range.

IV. DISCUSSION

In what follows, an effort is made to establish a quantitative relationship between the materials behavior and the

actuation behavior. The measured actuation strain is compared with that determined from Eq. (2) using material parameters determined independently as described in Secs. II and III. Equation (2) gives the actuation strain in thickness direction of the elastomer film. However, the in-plane radial strain, s, measured by the video extensometer in actuator measurements is derived from Eq. (2) assuming constant volume deformation and in-plane isotropy, so that

$$s = \frac{1}{\sqrt{1 + \frac{\varepsilon\varepsilon_0}{Y}E^2}} - 1. \tag{7}$$

For TPE and PDMS, the values for the dielectric constant given in Table II were assumed to be valid for all frequencies considered. The dielectric constant in VHB was determined from Eq. (3), with the fitting parameters in Table I.

Because the present work addresses only small strains, it is assumed that the compression modulus Y in Eq. (7) may be substituted by the initial (zero strain) value of Y_{stretch}. Moreover, it is assumed that the frequency dependence of Y is independent of strain and may hence be inferred from that of Y', given by Eq. (6). Y was therefore expressed in terms of Y_{stretch} determined from the tensile tests and a frequency factor F determined from the shear modulus data, i.e.,

$$Y(f,s) = F(f)Y_{\text{stretch}}(s). \tag{8}$$

F was determined by normalizing $Y'(f)$ with its value at 0.28 Hz $[F(f)=Y'(f)/Y'(f=0.28\ \text{Hz})]$, which was the nominal strain rate in the tensile tests.

The actuation strain was then calculated by combining Eqs. (3), (7), and (8). In Fig. 6 the calculated actuation strain (solid curves) is shown as a function of frequency and compared with the experimentally determined strain amplitude (symbols). The agreement between the calculated and the measured strain was generally satisfactory at low frequencies, bearing in mind the approximations inherent in the present approach. An attempt to improve the description of the VHB actuator was also made by taking into account the effect of strain hardening on Y_{stretch} [hatched line in Fig. 6(a)].

At frequencies above 50 mHz, the calculated curves overestimated the observed actuator response for all the materials, particularly for TPE. Thus, whereas the calculated strain of 2.79% for TPE at 1 mHz was comparable with the strain of 2.01% measured at the same frequency, the measured strain decreased to only 0.03% at 1 Hz as compared with a calculated value of 2.23%. This discrepancy could not be attributed to the electric circuit, whose RC time constant was determined to be of the order of 1 ms, and hence only to be significant for frequencies of 1 kHz or more. Rather, it was thought to reflect the assumption of a purely elastic materials response in the calculations. It may be inferred from Fig. 5 that viscous effects should become increasingly important at high frequencies, particularly since $\tan\varphi$ also increased with increasing frequency.

To provide direct measure of the materials actuator performance, an "actuation factor" A_f was defined from Eq. (2), such that

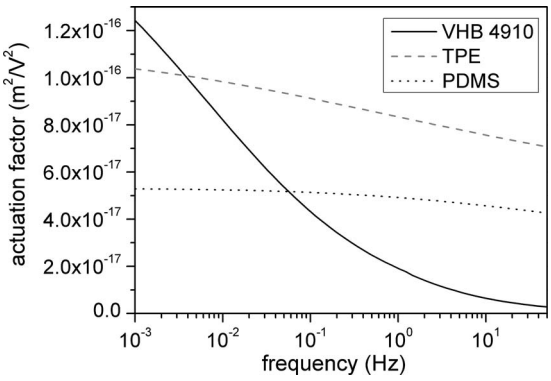

FIG. 7. Actuation factor A_f (quotient of dielectric constant and elastic modulus) as a function of frequency of applied electric field for the three elastomers.

$$s_z(f) = \frac{\varepsilon'(f)\varepsilon_0}{Y(f)}E^2 = -A_f(f)E^2. \tag{9}$$

The minus sign is included to receive positive values for A_f, as Y is negative (compression modulus). The A_f for the three elastomers are shown in Fig. 7 as a function of frequency. In each case, A_f decreased with frequency, but the strongest decrease was observed for VHB. Hence, although VHB showed the highest A_f of the three elastomers at frequencies up to 3.5 mHz, it showed the lowest A_f at frequencies greater than 55 mHz. Because there was little change in the dielectric properties in the frequency range considered, A_f is dominated by the mechanical response.

Thus, in terms of A_f, TPE outperformed VHB over nearly the whole frequency range, in spite of having a significantly lower dielectric constant (2 as compared with 4.65 for VHB), and it may be inferred from the even weaker dependence of A_f on frequency for PDMS that this latter material should continue to perform well up to still higher frequencies.

The results for VHB are consistent with those of Plante and Dubowsky,[17] who found that VHB actuators only work reliably when used for short time periods at high stretch rates, which is directly attributable to the strongly viscoelastic behavior of VHB, particularly at high frequencies. As the performance of VHB drops significantly under such conditions, this clearly limits the applicability of VHB actuators.

V. CONCLUSIONS

A quantitative description of the small strain response of DEAs at low frequencies was established, based on dielectric spectroscopy and dynamic mechanical analysis. The generality of this model was investigated by applying it to three different elastomers, all of which were well described, although viscoelastic losses and geometrical effects were not taken into account explicitly. This result is of interest for materials selection and development for DEA applications because it avoids the need for a strain energy function or calculations based on complex geometries, while demonstrating that independently determined material parameters may be used to predict the actuator performance for a given material.

The actuator performance in the frequency range investigated was found to be dominated by the frequency dependence of the elastic response and was less influenced by dielectric properties, the dielectric constant remaining roughly constant in all the materials over the frequency range considered.

An extension of this analysis to still higher frequencies may be possible by using time-temperature superposition.[18] However, for the analysis of higher actuation strains, it will be necessary to work with a charge controlled voltage source in order to ensure a constant electrostatic pressure during actuation, which is not possible with a voltage regulated power source.

ACKNOWLEDGMENTS

The authors gratefully acknowledge the financial support of EMPA (Project No. 841331) and the Austrian Science Fund (Project No. 20772-N20), Arne Schmidt, EMPA Dübendorf, for helpful discussions, and Martin Kaltenbrunner and Reinhard Schwödiauer, JKU Linz, for their technical assistance with the dielectric measurements.

[1] *Electroactive Polymers (EAP) as Artificial Muscles, Reality, Potential and Challenges*, edited by Y. Bar-Cohen (SPIE, Bellingham, WA, 2001).
[2] *Dielectric Elastomers as Electromechanical Transducers: Fundamentals, Materials, Devices, Models and Applications of an Emerging Electroactive Polymer Technology*, edited by F. Carpi D. de Rossi, R. Kornbluh, and P. Sommer-Larsen (Elsevier, Amsterdam, 2008).
[3] R. Pelrine, R. Kornbluh, Q. Pei, and J. Joseph, Science **287**, 836 (2000).
[4] R. Kornbluh, Mater. Technol. **19**, 216 (2004).
[5] R. Pelrine, R. Kornbluh, and J. Joseph, Sens. Actuators, A **64**, 77 (1998).
[6] G. Kofod and P. Sommer-Larsen, Sens. Actuators, A **122**, 273 (2005).
[7] F. Carpi and D. De Rossi, Mater. Sci. Eng., C **24**, 555 (2004).
[8] M. Wissler and E. Mazza, Sens. Actuators, A **134**, 494 (2007); **120**, 184 (2005); **14**, 1396 (2005).
[9] F. Carpi, G. Gallone, F. Galantini, and D. de Rossi, Adv. Funct. Mater. **18**, 235 (2008).
[10] R. Palakodeti and M. R. Kessler, Mater. Lett. **60**, 3437 (2006).
[11] ISO 37:2005(E), Rubber, vulcanized or thermoplastic—Determination of tensile stress-strain properties, 4th ed., 15 July 2005.
[12] F. Kremers and A. Schönhals, *Broadband Dielectric Spectroscopy* (Springer, Berlin, 2003).
[13] G. Kofod, P. Sommer-Larsen, R. Kornbluh, and R. Pelrine, J. Intell. Mater. Syst. Struct. **14**, 787 (2003).
[14] S. Havriliak and S. Negami, Polymer **8**, 161 (1967).
[15] A. K. Jonscher, Nature (London) **267**, 673 (1977).
[16] J. W. Fox and N. C. Goulbourne, J. Mech. Phys. Solids **56**, 2669 (2008); Proc. SPIE **6927**, 69271P (2008).
[17] J. S. Plante and S. Dubowsky, Int. J. Solids Struct. **43**, 7727 (2006).
[18] J. D. Ferry, *Viscoelastic Properties of Polymers* (Wiley, New York, 1980).